Proton radioactivity within a generalized liquid drop model

J.M. Dong, H.F. Zhang, Guy Royer

Proton radioactivity within a generalized liquid drop model

J. M. Dong,[1] H. F. Zhang,[1] and G. Royer[2]

[1]*School of Nuclear Science and Technology, Lanzhou University, Lanzhou 730000, China*
[2]*Laboratoire Subatech, UMR: IN2P3/CNRS-Université-Ecole des Mines, Nantes 44, France*

(Dated: June 2, 2009)

The proton radioactivity half-lives of spherical proton emitters are investigated theoretically. The potential barriers preventing the emission of proton are determined in the quasimolecular shape path within a generalized liquid drop model (GLDM) including the proximity effects between nuclei in a neck and the mass and charge asymmetry. The penetrability is calculated in the WKB approximation. The spectroscopic factor has been taken into account in half-life calculation, which is obtained by employing the relativistic mean field (RMF) theory combined with the BCS method with the force NL3. The half-lives within the GLDM are compared with the experimental data and other theoretical values. GLDM works quite well for spherical proton emitters when the spectroscopic factors are considered, indicating the necessity of introducing the spectroscopic factor and the success of the GLDM for proton emission. Finally, we present two formulae for proton emission half-life similar to the Viola-Seaborg formulae and Royer's formulae of α-decay.

PACS numbers: 23.50.+z, 21.10.Tg, 21.10.Jx, 21.60.-n

I. INTRODUCTION

The opportunities provided by the radioactive beam facilities make the study of the exotic nuclei with extreme numbers of neutrons or protons a very interesting topic both from the experimental and theoretical points of view. And studies on these exotic nuclei lead to the discovery of a new form of radioactivity-proton emission. The proton drip line represents one of the fundamental limits of nuclear existence and the nucleus with a very large excess of protons undergo spontaneous proton emission towards stability. Besides, the rapid proton capture process which plays a very important role in nuclear astrophysics has its inverse in the proton radioactivity from the nuclear ground state or low isomeric states. Therefore the study of the proton emission is significative. This proton emission from nuclei was firstly observed in an isomeric state of ^{53}Co in 1970. With the development of experimental facilities and radioactive beams, proton emissions from ground state or low isomeric states have been identified between $Z = 51$ and $Z = 83$ [1] and more proton-emitting nuclei will be observed in experiments in the future.

The proton radioactivity can be used as an useful tool to extract nuclear structure information such as the shell structure and the coupling between bound and unbound nuclear states [2]. Measurement on the proton energy, half-life and proton branching ratio (fine structure) helps to determine the angular momentum l carried away by the emitted proton and to characterize its wave function inside the nucleus [1, 3, 4]. The proton emission can be dealt with in the framework of WKB barrier penetration model since the decay process can be treated in a simple quantum tunneling effect through a potential barrier. Several approaches have been employed to study the half-lives of spherical proton emitters, such as the distorted-wave Born approximation [5], the density-dependent M3Y(DDM3Y) effective interaction [6, 7], JLM interaction [7], and the unified fission model [8]. However, the calculations in Ref. [6, 7, 8] did not take account the spectroscopic factor. The spectroscopic factor is very important from the viewpoint of the nuclear structure. In this study, we calculate the spectroscopic factor by employing the relativistic mean field theory in combination with the BCS method, and then determine the partial proton emission half-lives of spherical proton emitters within the macro-microscopic GLDM. The calculated results are compared with the experimental data and other theoretical results.

The paper is organized as follows. In Sec. II, the framework of GLDM and the method for spectroscopic factor are presented. The calculated proton emission half-lives are shown and discussed in Sec. III. In Sec. IV, two formulae for proton emission are proposed. Finally, we present a brief summary of the present work.

II. METHODS

The GLDM allows to describe the processes of fusion, fission, light nucleus and α emission [9, 10, 11, 12, 13, 14, 15, 16, 17]. The macroscopic energy includes the volume, surface, Coulomb and proximity energies:

$$E = E_V + E_S + E_C + E_{\rm Prox}. \tag{1}$$

For one-body shapes, the volume, surface and Coulomb energies are given by:

$$E_V = -15.494(1 - 1.8I^2)A \text{ MeV}, \tag{2}$$

$$E_S = 17.9439(1 - 2.6I^2)A^{2/3}(S/4\pi R_0^2) \text{ MeV}, \tag{3}$$

$$E_C = 0.6e^2(Z^2/R_0)\times 0.5\int (V(\theta)/V_0)(R(\theta)/R_0)^3 \sin\theta d\theta. \tag{4}$$

I is the relative neutron excess and S is the surface area of the one-body deformed nucleus. $V(\theta)$ is the electrostatic potential at the surface and V_0 the surface potential of the sphere. When the nuclei are separated :

$$E_V = -15.494\left[(1-1.8I_1^2)A_1+(1-1.8I_2^2)A_2\right]\ \text{MeV}, \tag{5}$$

$$E_S = 17.9439\left[(1-2.6I_1^2)A_1^{2/3}+(1-2.6I_2^2)A_2^{2/3}\right]\ \text{MeV}, \tag{6}$$

$$E_C = 0.6e^2Z_1^2/R_1 + 0.6e^2Z_2^2/R_2 + e^2Z_1Z_2/r. \tag{7}$$

The additional centrifugal energy E_l coming from the angular momentum of the emitted proton has been introduced:

$$E_l(r) = \frac{\hbar^2}{2\mu}\frac{l(l+1)}{r^2}. \tag{8}$$

Here A_i, Z_i, R_i and I_i are the mass number, charge number, radii and relative neutron excesses of the two nuclei. The relative neutron excess of a proton is fixed at $I_2 = 0$ to ensure a negative volume energy and a positive surface energy. The dimensionless quantity of l is the angular momentum carried by the emitted proton(angular momentum transfer). μ is the reduced mass. r is the distance between the mass centers. The radii R_i of the daughter nucleus and proton are given by [13]:

$$R_i = (1.28A_i^{1/3} - 0.76 + 0.8A_i^{-1/3})\ \text{fm}, i = 1, 2. \tag{9}$$

The radii R_0 of parent nucleus can be obtained with the volume conservation:

$$R_0^3 = R_1^3 + R_2^3. \tag{10}$$

The surface energy results from the effects of the surface tension forces in a half space. The nuclear proximity energy E_{prox} has been introduced to take into account the additional surface effects due to the attractive nuclear forces between the surfaces in a neck or a gap between two separated fragments:

$$E_{\text{Prox}}(r) = 2\gamma\int_{h_{\min}}^{h_{\max}}\Phi\left[D(r,h)/b\right]2\pi h dh, \tag{11}$$

where h is the distance varying from the neck radius or zero to the height of the neck border. D is the distance between the surfaces in regard and $b = 0.99$ fm is the surface width. Φ is the proximity function of Feldmeier [18] and the surface parameter γ is the geometric mean between the surface parameters of the two nuclei or fragments:

$$\gamma = 0.9517\sqrt{(1-2.6I_1^2)(1-2.6I_2^2)}\ \ \text{MeV}\cdot\text{fm}^{-2}. \tag{12}$$

The partial half-life of a spherical proton emitter is calculated using the WKB barrier penetration probability. The decay constant of the proton emitter is simply defined as $\lambda = \nu_0 P S_{\text{p}}$ and half-life $T_{\text{p}} = \ln 2/\lambda$. The assault frequency ν_0 has been taken as $8\times10^{20}\ \text{s}^{-1}$. The barrier penetrability P is calculated by the following formula:

$$P = \exp\left[-\frac{2}{\hbar}\int_{R_{\text{in}}}^{R_{\text{out}}}\sqrt{2B(r)(E(r)-E(\text{sphere}))}dr\right]. \tag{13}$$

where R_{in} and R_{out} are the two turning points of the WKB action integral. The two following approximations are used here: $R_{\text{in}} = R_1 + R_2$ and $B(r) = \mu$. R_{out} is given as:

$$R_{\text{out}} = \frac{Z_1Z_2e^2}{2Q} + \sqrt{\left(\frac{Z_1Z_2e^2}{2Q}\right)^2 + \frac{l(l+1)\hbar^2}{2\mu Q}}. \tag{14}$$

For proton radioactivity, the spectroscopic factor is given by [5, 19]:

$$S_{\text{p}} = u_j^2, \tag{15}$$

where u_j^2 is the probability that the spherical orbit of emitted proton is empty in the daughter nucleus. Fortunately, the daughter nuclei of spherical proton emitters are all in ground states. Thus, it is relatively easy to determine this spectroscopic factor by using the RMF theory combined with the BCS method. The RMF automatically includes the spin-orbit interaction. It has received much attention due to its great success in describing the structure of the stable nuclei [20], neutron-rich nuclei [21], proton-rich nuclei [22], superdeformed nuclei [23] and superheavy nuclei [24, 25, 26] . It is now a standard tool in low energy nuclear structure. The RMF theory is well known and it will not be discussed in detail here. The pairing correlation is treated by the BCS method. We have introduced the strength of the pairing forces in the following forms for neutrons and protons, respectively [26]:

$$G_{\text{n}} = \frac{21}{A}(1-\frac{N-Z}{2A})\ \ \text{MeV}\ , \tag{16}$$

$$G_{\text{p}} = \frac{27}{A}(1+\frac{N-Z}{2A})\ \ \text{MeV} \tag{17}$$

which depend on the proton number Z and neutron number N. A is the total mass number. The NL3 parameter set, which has been used with enormous success in the description of a variety of ground-state properties of spherical, deformed and exotic nuclei [27, 28], is used here. Unlike the situation near the neutron drip line, for proton-rich nuclei the Coulomb barrier confines the protons in the interior of the nucleus. As a consequence, the effects of the coupling to the continuum is weaker and therefore for nuclei close to proton drip line, the RMF+BCS model could still be considered as a reasonable approximation providing sufficiently accurate results [22].

III. HALF-LIVES OF SPHERICAL PROTON EMITTERS

The values of angular momentum transfer l, decay energy Q, penetrability P, spectroscopic factor $S_{\rm p}$, the experimental and calculated proton emission half-life are given in Table I. The experimental Q value, which is a crucial quantity to determine the decay half-life, is used for the calculation and the potential barrier given by the GLDM has been adjusted to reproduce the experimental Q value.

In Ref. [6], D. N. Basu and coworkers calculated the half-lives of spherical proton emitters using the density-dependent M3Y effective interaction with the density of the daughter nucleus taking from phenomenological models. Madhubrate Bhattacharya and G. Gangopadhyay developed this model by obtaining this density from mean field calculation and also used the JLM effective interaction [7]. The results have been presented in the last three columns of Table I for comparison. As can be seen, The DDM3Y and JLM models can provide good explanation for most cases. Their is no doubt that the DDM3Y and JLM models are very successful because their microscopic nature includes many nuclear features. In a number of decays, however, the results do not match so well, such as ^{147}Tm, ^{150}Lu, ^{156}Ta and ^{156}Ta(isomeric state). For ^{177}Tl(isomeric state) and ^{185}Bi, the discrepancies are off by an order of magnitude compared with the experimental data. It is their calculations without introducing the spectroscopic factor that leads to a large deviation for some nuclei. In order to obtain more information about proton-radioactivity and preform more accurate investigation theoretically, we calculated the spectroscopic factor within the RMF+BCS, and the results are shown in the fifth column of Table I. One could notice that, spectroscopic factor is $S_{\rm p} \sim 1$ at the beginning of a proton shell of residual daughter nucleus, but moving away, it decreases, becoming quite small at the end of the shell. This shows the shell structure plays an important role for the spectroscopic factor. Hence the spectroscopic factor includes the shell effect to a large extent. For ^{177}Tl (isomeric state) and ^{185}Bi, the spectroscopic factors are very small, leading to the longer half-lives than the DDM3Y and JLM calculated.

We calculate the half-lives by employing the GLDM taking account the spectroscopic factors. The penetration probabilities obtained with GLDM are shown in the fourth column. The penetrability P stay between 10^{-23} and 10^{-16} which are relatively very large while the range is narrow, compared with $10^{-39} \sim 10^{-14}$ for α-decay [29]. Hence it is easy for the proton to escape from the proton emitter, confirming that the proton-emitting nuclei are weakly bound. The calculated half-lives are presented in the seventh column. The half-lives by the GLDM with the average discrepancy less than 40%, give better agreement with the experimental data than that by DDM3Y and JLM models. For nuclei ^{147}Tm, ^{150}Lu, ^{156}Ta, ^{156}Ta(isomeric state) and ^{177}Tl(isomeric state), which the DDM3Y and JLM can not explain well, the GLDM could give a very excellent results with the deviation 4%, 26%, 5%, 10% and 33% respectively. This indicates that the including of the spectroscopic factors in calculations is necessary. The quantitative agreement with the experimental data are better than other theoretical ones which demonstrates that the GLDM with the proximity effects, centrifugal potential energy, the mass asymmetry and spectroscopic factor could be used to investigate the proton emission successfully when the right Q values are given. The GLDM overestimates the half-life of ^{185}Bi by one order of magnitude. The first reason possibly is the uncertainty of the Q value or the emitted proton being not in $s_{1/2}$ state, and it requires further investigation theoretically and measurements with high accuracy. The second reason is, perhaps, the shell effect is not included in the potential barrier, though the most shell effect contribution has been included in the Q value and spectroscopic factor. It is sure that the GLDM connected with WKB approximation will quantitatively give more consistent results for the proton radioactivity half-life when the shell effect is included in the penetration barrier.

Recently, the spherical proton emitter ^{155}Ta was observed. Its emitted proton energy and half-life have been measured again [30]. With the angular momentum transfer $l = 5$ [31] and proton energy $E_{\rm p} = 1.444 \pm 0.015$ MeV ($Q = 1.453 \pm 0.015$ MeV), we obtain half-life of $T_{\rm p} = 3.9^{+1.4}_{-1.0}$ ms using the GLDM compared with the experimental data of $T_{\rm p} = 2.9^{+1.5}_{-1.1}$ ms. The Q value is compatible with the half-life, indicating the experimental data should be reliable. The new spherical proton emitter ^{159}Re was synthesized in the reaction ^{106}Cd (^{58}Ni, p4n) ^{159}Re [32] and its proton emission Q value along with half-life have been measured recently. The Q value is compatible with the half-life if and only if $l = 5$ (the calculated value is 23^{+8}_{-6} μs in contrast with the experimental data of 21^{+4}_{-4} μs), which indicates the proton is emitted from an $\pi h_{11/2}$ state agreeing with the conclusion in Ref. [32].

IV. NEW FORMULAS FOR PROTON EMISSION HALF-LIFE

The centrifugal potential energy E_l can reduce the tunneling probability and hence increases the half-life. A formula can be deduced to describe this relationship between half-life and l value for proton emission, being similar to the formula for α-decay in Ref. [33]:

$$\log_{10} T_{\rm p}(l) = \log_{10} T_{\rm p}(0) + c_0 \frac{l(l+1)}{\sqrt{(A-1)(Z-1)A^{-2/3}}}. \quad (18)$$

The half-life $T_{\rm p}$ is measured in second. c_0 is slightly model dependent with $c_0 = 2.5$ for the GLDM. With the formula (18), we fit new formulae that could be used to describe half-life for proton emission. A formula is

proposed in the following form:

$$\log_{10}[T_{\rm p}({\rm s})] = (aZ+b)Q^{-1/2}+c+ c_0\frac{l(l+1)}{\sqrt{(A-1)(Z-1)A^{-2/3}}}, \quad (19)$$

where Z and A are charge and mass numbers of the parent nucleus respectively, and Q the proton decay energy in MeV. The first two terms are similar to Viola-Seaborg formulae [34, 35] for α-decay and the last term is exactly the contribution of centrifugal barrier from formula (18). Performing a least squares fit to the half-lives of first 25 spherical proton emitters available in Table I, we obtain a set of parameters for formula (19). There values are: $a = 0.3437$, $b = 4.9628$, $c = -31.1253$ and $c_0 = 2.5950$, with the average deviation $\overline{\sigma}$=0.153 between the experimental and formula. Additionally, we obtained a set of parameters for half-lives of deformed proton emitters by employing a least squares fit to data, which include 11 nuclei ($Z = 53-67$) that could be found in literature [1] or [31]. These parameters are: $a = 0.3637$, $b = 4.6467$, $c = -30.9299$ and $c_0 = 2.6244$. The average deviation is $\overline{\sigma} = 0.323$. The half-life increases by 3$\sim$4 orders of magnitude when the angular momentum transfer l is changed from zero to five in terms of this formula. In other words, the half-life of proton emission is quite sensitive to the angular momentum l of the emitted proton, which in turn helps to determine the l value when half-life and Q value are measured. On the other hand, so many proton emitters have been observed in experiments at present due to the centrifugal barriers prolonging lifetimes of these nuclei to a great extent.

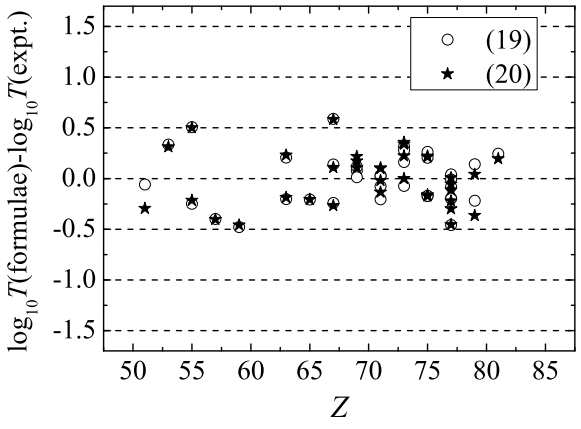

FIG. 1: Deviation between the formulae (19,20) and experimental logarithm of half-lives for proton emission.

The other formula for proton emission is given by

$$\log_{10}[T_{\rm p}({\rm s})] = a+bA^{1/6}\sqrt{Z}+cZQ^{-1/2}+ c_0\frac{l(l+1)}{\sqrt{(A-1)(Z-1)A^{-2/3}}}. \quad (20)$$

The first three terms are similar to Royer's formulae for α-decay [16, 36]. With the same method we discussed above, we obtained the parameter sets: $a = -23.0632$, $b = -0.4225$, $c = 0.4170$ and $c_0 = 2.5989$ for spherical proton emitters with average deviation $\overline{\sigma} = 0.183$; $a = -23.9341$, $b = -0.3936$, $c = 0.4385$ and $c_0 = 2.6167$ for deformed proton emitters with $\overline{\sigma} = 0.316$. The two formulae (19,20) can validate each other, and get the more reliable results in future study. The experimental proton radioactivity half-lives of most nuclei can be reproduced within a factor of less than 2 by the above two formulae. The little discrepancy suggests that these two formulae could be used to determine the l value when Q and $T_{\rm p}$ values have been measured and then extract some useful information about nuclear structure as well as to calculate proton emission half-lives. The proton and α emission can be described by the similar formulae with the different parameters, which is exactly what we expect. Since both the two decay modes are quantum tunneling effect, the studies on them should be unified.

From these two formula, it is easy to deduce the following equation:

$$\frac{\partial(\log_{10}T_{\rm p})}{\partial Q} = -\frac{1}{2}(aZ+b)Q^{-3/2}, \text{ or } -\frac{1}{2}cZQ^{-3/2}, \quad (21)$$

which reflects the Q value dependence of half-life. By comparing these parameters and Q values with that in Viola-Seaborg and Royer's formulae for α-decay, one could find that the half-life is more sensitive to Q value for proton emission. In addition, $C_0 \approx 2.6$ for proton emission in contrast with $C_0 = 1.0$ [33] for α-decay indicates that the centrifugal barrier is much more important for proton emission than that for α-decay, due to smaller reduced mass μ (and hence the high centrifugal barrier) compared with that in α-decay system. These imply that it is quite difficult to predict the half-life of proton emission for unknown nucleus since the Q value can not be obtained with a good accuracy and since the uncertainty on the l value is large.

V. SUMMARY

The proton radioactivity of spherical proton emitters has been analyzed in the framework of the GLDM for the first time. The penetration barriers are constructed in the quasimolecular shape path, and the penetration probabilities are calculated with the WKB approximation. The penetration probabilities are relatively very large while its range is narrow. Therefore it is easy for the proton to escape from the proton emitter, confirming the proton emitting nuclei are weakly bound. The

spectroscopic factors have been taken into account in half-lives calculations, which are obtained by employing the relativistic mean field theory combined with the BCS method. The spectroscopic factor is affected greatly by the proton shell structure, and in turn it contains shell effect to a large extent. For ^{177}Tl (isomeric state) and ^{185}Bi, the spectroscopic factors are very small (0.022 and 0.011), leading to the longer half-lives than the DDM3Y and JLM calculated. Although the DDM3Y and JLM models include the appropriate considerations in the microscopic level, the present calculations are better agreement with the experimental data than that within the DDM3Y and JLM models. This, indicates the considering of spectroscopic factor is necessary for proton emission, especially for the nuclei with residual daughter nuclei at the end of the shell. Additionally, some newly observed proton emitters ^{155}Ta and ^{159}Re have been analyzed. Finally, two formulae similar to Viola-Seaborg formulae and Royer's formulae have been proposed for proton radioactivity. On the one hand, they can be employed to calculate the proton emission half-life. On the other hand, they can be used to determine the l value when the Q value and half-life have been measured and then extract some useful information about nuclear structure since the decay rate is quite sensitive to l value. The proton and α emission can be described by the similar formulae with different parameters, but the half-life of proton radioactivity is more sensitive to Q and l values compared with α-decay according to our analysis, leading to the prediction of the half-lives for proton emission quite difficult.

Acknowledgements

This work is supported by the Natural Science Foundation of China (grants 10775061, and 10805016); by the Fundamental Research Fund for Physics and Mathematics of Lanzhou University(grants LZULL200805); by the CAS Knowledge Innovation Project NO.KJCX-SYW-N02; The Major State Basic Research Developing Program of China (2007CB815004).

[1] A. A. Sonzogni, Nuclear Data Sheets **95**, 1 (2002).
[2] M. Karny, K. P. Rykaczewski, R. K. Grzywacz, J. C. Batchelder, C. R. Bingham, C. Goodin, C. J. Gross, J. H. Hamilton, A. Korgul, W. Królas, S. N. Liddick, K. Li, K. H. Maier, C. Mazzocchi, A. Piechaczeki, K. Rykaczewski, D. Schapira, D. Simpson, M. N. Tantawy, J. A. Winger, C. H. Yu, E. F. Zganjar, N. Nikolov, J. Dobaczewski, A. T. Kruppa, W. Nazarewicz, M. V. Stoitsov, Phys. Lett. **B664**, 52 (2008).
[3] A. T. Kruppa, W. Nazarewicz, Phys. Rev. C **69**, 054311 (2004).
[4] L. S. Ferreira, M. C. Lopes, E. Maglione, Prog. Part. Nucl. Phys. **59**, 418 (2007).
[5] S. Aberg, P. B. Semmes and W. Nazarewicz, Phys. Rev. C **56**, 1762 (1997).
[6] D. N. Basu, P. Roy Chowdhury, C. Samanta, Phys. Rev. C **72**, 051601(R) (2005) .
[7] M. Bhattacharya and G. Gangopadhyay, Phys. Lett. **B651**, 263 (2007).
[8] M. Balasubramaniam and N. Arunachalam, Phys. Rev. C **71**, 014603 (2005).
[9] G. Royer, B. Remaud, J. Phys. G: Nucl. Part. Phys. **10**, 1057 (1984).
[10] G. Royer, B. Remaud, Nucl. Phys. **A444**, 477 (1985).
[11] G. Royer, J. Phys. G: Nucl. Part. Phys. **26**, 1149 (2000).
[12] G. Royer, R. Moustabchir, Nucl. Phys. **A683**, 182 (2001).
[13] G. Royer, R. A. Gherghescu, Nucl. Phys. **A699**, 479 (2002) .
[14] G. Royer, K. Zbiri, C. Bonilla, Nucl. Phys. **A730**, 355 (2004).
[15] H. F. Zhang, W. Zuo, J. Q. Li and G. Royer, Phys. Rev. C **74**, 017304 (2006).
[16] G. Royer and H. F. Zhang, Phys. Rev. C **77**, 037602 (2008).
[17] J. M. Dong, H. F. Zhang, W. Zuo, J. Q. Li, Chin. Phys. Lett. **25**, 4230 (2008).
[18] H. Feldmeier, 12th Summer School on Nuclear Physics, Mikolajki, Poland, 1979.
[19] D. S. Delion, R. J. Liotta, R. Wyss, Phys. Rep. **424**, 113 (2006).
[20] G. Gangopadhyay, Phys. Rev. C **59**, 2541 (1999).
[21] J. Meng, H. Toki, S. G. Zhou, S. Q. Zhang, W. H. Long, L. S. Geng, Prog. Part. Nucl. Phys. **57**, 470 (2006).
[22] G. A. Lalazissisand S. Raman, Phys. Rev. C **58**, 1467 (1998).
[23] J. König and P. Ring, Phys. Rev. Lett. **71**, 3079 (1993).
[24] Z. Z. Ren, Phys. Rev. C **65**, 051304(R) (2002).
[25] S. Das and G. Gangopadhyay, J. Phys. G: Nucl. Part. Phys. **30**, 957 (2004).
[26] H. F. Zhang, J. Q. Li, W. Zuo, Z. Y. Ma, B. Q. Chen, and S. Im, Phys. Rev. C **71**, 054312 (2005); J. Q. Li, Z. Y. Ma, B. Q. Chen, and Y. Zhou, Phys. Rev. C **65**, 064305 (2002).
[27] B. G. Todd-Rutel and J. Piekarewicz, Phys. Rev. Lett. **95**, 122501 (2005).
[28] G. Lalazissis, J. König, and P. Ring, Phys. Rev. C **55**, 540 (1997).
[29] H. F. Zhang and G. Royer, Phys. Rev. C **77**, 054318 (2008).
[30] R. D. Page, L. Bianco, I. G. Darby, J. Uusitalo, D. T. Joss, T. Grahn, R.-D. Herzberg, J. Pakarinen, J. Thomson, S. Eeckhaudt, P. T. Greenlees, P. M. Jones, R. Julin, S. Juutinen, S. Ketelhut, M. Leino, A.-P. Leppänen, M. Nyman, P. Rahkila, J. Sarén, C. Scholey, A. Steer, M. B. Gómez Hornillos, J. S. Al-Khalili, A. J. Cannon, P. D. Stevenson, S. Ertürk, B. Gall, B. Hadinia, M. Venhart, and J. Simpson , Phys. Rev. C **75**, 061302(R) (2007).
[31] D. S. Delion, R. J. Liotta and R. Wyss, Phys. Rev. Lett. **96** 072501 (2006).

[32] D. T. Joss, I. G. Darby, R. D. Page, J. Uusitalo, S. Eeckhaudt, T. Grahn, P. T. Greenlees, P. M. Jones, R. Julin, S. Juutinen, S. Ketelhut, M. Leino, A.-P. Leppänenc, M. Nyman, J. Pakarinen, P. Rahkila, J. Sarén, C. Scholey, A. Steer, A. J. Cannon, P. D. Stevenson, J. S. Al-Khalili, S. Ertürk, M. Venhart, B. Gall, B. Hadinia, J. Simpson, Phys. Lett. **B641**, 34 (2006).

[33] J. M. Dong (private communication, 2009).

[34] P. Möller, J. R. Nix and K. -L. Kratz, Atomic Data and Nuclear Data Tables **66**, 131 (1997).

[35] C. Samanta, P. Roy Chowdhury, D. N. Basu, Nucl. Phys. **A789**, 142 (2007).

[36] R. Moustabchir, G. Royer, Nucl. Phys. **A683**, 266 (2001).

TABLE I: Comparison between experimental and calculated proton radioactivity logarithmic half-lives of spherical proton emitters. The asterisk(*) symbols in parent nuclei denote the isomeric states. The experimental data of ^{155}Ta and ^{159}Re are taken from Ref. [30] and Ref. [32], respectively and their Q values are calculated using the measured emitted proton energies. Other experimental data are from Ref. [1].

Parent	l	Q(MeV) expt.	Penetrability	$S_{\rm p}$	$\log_{10} T_{\rm p}$(s) expt.	$\log_{10} T_{\rm p}$(s) GLDM	$\log_{10} T_{\rm p}$(s) DDM3Y[6]	$\log_{10} T_{\rm p}$(s) DDM3Y[7]	$\log_{10} T_{\rm p}$(s) JLM[7]
^{105}Sb	2	0.491	1.280×10^{-23}	0.999	2.049	1.831	1.97	2.27	1.69
^{145}Tm	5	1.753	6.759×10^{-16}	0.580	-5.409	-5.656	-5.14	-5.20	-5.10
^{147}Tm	5	1.071	3.931×10^{-22}	0.581	0.591	0.572	0.98	0.98	1.07
^{147}Tm*	2	1.139	2.504×10^{-18}	0.953	-3.444	-3.440	-3.39	-3.26	-3.27
^{150}Lu	5	1.283	3.554×10^{-20}	0.497	-1.180	-1.309	-0.58	-0.59	-0.49
^{150}Lu*	2	1.317	5.734×10^{-17}	0.859	-4.523	-4.755	-4.38	-4.24	-4.24
^{151}Lu	5	1.255	1.839×10^{-20}	0.490	-0.896	-1.017	-0.67	-0.65	-0.55
^{151}Lu*	2	1.332	8.262×10^{-17}	0.858	-4.796	-4.913	-4.88	-4.72	-4.73
^{155}Ta	5	1.453	5.280×10^{-19}	0.422	-2.538	-2.410	-4.65	-4.67	-4.57
^{156}Ta	2	1.028	4.994×10^{-21}	0.761	-0.620	-0.642	-0.38	-0.22	-0.23
^{156}Ta*	5	1.130	1.793×10^{-22}	0.493	0.949	0.991	1.66	1.66	1.76
^{157}Ta	0	0.947	1.608×10^{-21}	0.797	-0.523	-0.170	-0.43	-0.21	-0.23
^{159}Re	5	1.816	1.216×10^{-16}	0.308	-4.678	-4.636	–	–	–
^{160}Re	2	1.284	2.204×10^{-18}	0.507	-3.046	-3.111	-3.00	-2.86	-2.87
^{161}Re	0	1.214	2.024×10^{-18}	0.892	-3.432	-3.319	-3.46	-3.28	-3.29
^{161}Re*	5	1.338	1.419×10^{-20}	0.290	-0.488	-0.677	-0.60	-0.57	-0.49
^{164}Ir	5	1.844	7.542×10^{-17}	0.188	-3.959	-4.214	-3.92	-3.95	-3.86
^{165}Ir*	5	1.733	1.335×10^{-17}	0.187	-3.469	-3.460	-3.51	-3.52	-3.44
^{166}Ir	2	1.168	2.624×10^{-20}	0.415	-0.824	-1.099	-1.11	-0.96	-0.96
^{166}Ir*	5	1.340	4.887×10^{-21}	0.188	-0.076	-0.025	0.21	0.22	0.30
^{167}Ir	0	1.086	1.126×10^{-20}	0.912	-0.959	-1.074	-1.27	-1.05	-1.07
^{167}Ir*	5	1.261	6.559×10^{-22}	0.183	0.875	0.858	0.69	0.74	0.81
^{171}Au	0	1.469	7.608×10^{-17}	0.848	-4.770	-4.872	-5.02	-4.84	-4.86
^{171}Au*	5	1.718	4.101×10^{-18}	0.087	-2.654	-2.613	-3.03	-3.03	-2.96
^{177}Tl	0	1.180	1.324×10^{-20}	0.733	-1.174	-1.049	-1.36	-1.17	-1.20
^{177}Tl*	5	1.986	1.166×10^{-16}	0.022	-3.347	-3.471	-4.49	-4.52	-4.46
^{185}Bi	0	1.624	1.942×10^{-16}	0.011	-4.229	-3.392	-5.44	-5.33	-5.36